Entropy squeezing and atomic inversion in the k-photon Jaynes–Cummings model in the presence of the Stark shift and a Kerr medium: A full nonlinear approach

H R Baghshahi[a)b)c)], M K Tavassoly[a)b)d)†], and A Behjat[a)d)]

[a)] *Atomic and Molecular Group, Faculty of Physics, Yazd University, Yazd, Iran*
[b)] *The Laboratory of Quantum Information Processing, Yazd University, Yazd, Iran*
[c)] *Department of Physics, Faculty of Science, Vali-e-Asr University of Rafsanjan, Rafsanjan, Iran*
[d)] *Photonics Research Group, Engineering Research Center, Yazd University, Yazd, Iran*

(Received 25 June 2013; revised manuscript received 28 November 2013; published online 15 May 2014)

The interaction between a two-level atom and a single-mode field in the k-photon Jaynes–Cummings model (JCM) in the presence of the Stark shift and a Kerr medium is studied. All terms in the Hamiltonian, such as the single-mode field, its interaction with the atom, the contribution of the Stark shift and the Kerr medium effects are considered to be f-deformed. In particular, the effect of the initial state of the radiation field on the dynamical evolution of some physical properties such as atomic inversion and entropy squeezing are investigated by considering different initial field states (coherent, squeezed and thermal states).

Keywords: Jaynes–Cummings model, entropy squeezing, atomic inversion, intensity-dependent coupling

PACS: 42.50.–p, 89.70.Cf, 42.50.Ct, 42.50.Dv **DOI:** 10.1088/1674-1056/23/7/074203

1. Introduction

The well-known Jaynes–Cummings model (JCM) is an important, simplified and standard model that elegantly describes the interaction between an atom and a single-mode field in the dipole and the rotating wave approximations (RWA).[1] Many interesting physical features have been studied with this model. Some examples include atomic inversion,[2] collapse and revival,[3,4] entanglement,[5–7] sub-Poissonian statistics,[8,9] quadrature squeezing[10] and entropy squeezing.[11,12] Many researches in this field are based on the linear interaction between atom and field, i.e., the atom–field coupling is assumed to be constant throughout the evolution of the whole system. Phoenix and Knight[13] used the JCM and employed a diagonalised reduced density operator to calculate the entropy and thereby demonstrated the essential two-state nature of the field. Kayham investigated the entropy squeezing of a two-level atom interacting with a quantum field prepared initially in the Glauber–Lachs state by using the standard JCM.[14] Liao *et al.* considered a system of two two-level atoms interacting with a binomial field in an ideal cavity and investigated the time evolution of the single-atom entropy squeezing, atomic inversion and linear entropy of the system.[15] Zhang *et al.* discussed the entanglement and the evolution of some of the nonclassicality features of the atom–field system in a standard JCM with squeezed vacuum and coherent state fields as the initial field state.[16] Mortezapour *et al.* studied the entanglement of a dressed atom and its spontaneous emission in a three-level Λ-type closed-loop atomic system under the multi-photon resonance condition and beyond it.[17] The entropy squeezing, atomic inversion and variance squeezing in the interaction between a two-level atom and a single mode cavity field via a k-photon process have been investigated in Ref. [18]. Ateto extended the JCM for the combined influences of a field-mode structure and a Kerr-like medium on the dynamics of entropy of entanglement of the cavity and atomic populations.[19]

However, in recent years, research has strongly focused on the nonlinear interaction between a two-level atom and a field in the deformed JCM. This model, which was firstly suggested by Buck and Sukumar,[20,21] describes the dependence of the atom–field coupling on the light intensity. Bužek investigated the physical quantities, particularly the atomic population and squeezing, in the intensity-dependent coupling JCM.[22] The interaction between a Λ-type three-level atom and a single-mode cavity field with intensity-dependent coupling in a Kerr medium has been investigated by one of the authors.[23] Sanchez and Récamier introduced a nonlinear JCM constructed from the standard structure by deforming all of the bosonic field operators.[24] Naderi *et al.* replaced $\hat{a}$ and $\hat{a}^\dagger$ in the standard JCM by the f-deformed operators $\hat{A}$ and $\hat{A}^\dagger$ and introduced a two-photon q-deformed JCM.[25] Barzangeh *et al.* investigated the effect of a classical gravitational field on the dynamical behavior of the nonlinear atom–field interaction within the framework of the f-deformed JCM.[26] Abdel-Aty *et al.* studied the entropy squeezing of a two-level atom in a Kerr medium and examined the influence of the nonlinear

†Corresponding author. E-mail: mktavassoly@yazd.ac.ir

© 2014 Chinese Physical Society and IOP Publishing Ltd

interaction of the Kerr medium on the quantum information and entropy squeezing.[27] Cordero and Récamier considered a Jaynes–Cummings Hamiltonian with deformed operators of the field and an additional Kerr term introduced by means of a purely algebraic method.[28] Recently, Faghihi *et al.* investigated the entanglement dynamics of the nonlinear interaction between a three-level atom (in a Λ configuration) and a two-mode cavity field in the presence of a cross-Kerr medium and its deformed counterpart,[29] intensity-dependent atom–field coupling and the detuning parameters.[30,31] The authors have also studied a three-level atom in motion which interacts with a single-mode field in an optical cavity in an intensity-dependent coupling regime.[32] The effects of the mean photon number, detuning, Kerr-like medium and various types of intensity-dependent couplings on the entanglement in the interaction between a Λ-type three-level atom and a two-mode field have been studied in Ref. [33].

Abdalla *et al.* considered the interaction of a two-level atom with a single-mode multi-photon field in a medium consisting of the Stark shift and the Kerr medium effects, with the coupling term assumed to be a function of time but still linear with the intensity of light.[34] Moreover, it is (partially) nonlinear only due to the presence of the Kerr medium. They investigated atomic inversion and entropy squeezing and showed that, the existence of the time-dependent coupling parameter leads to a time delay in the interaction which is twice the delay for the time-independent case. The aim of the present paper to nonlinearize the atom–field system considered in Ref. [34]. Precisely speaking, the interaction will occur in a time-dependent and at the same time nonlinear manner between a two-level atom and a nonlinear single-mode field for k-photon transitions in the presence of the Stark shift effect and the Kerr medium, both of which are considered to be f-deformed. As is clear, in this way, all terms in the Hamiltonian will be in a nonlinear regime by including a nonlinearity function $f(n)$, which is generally a well-defined function of the intensity of light. Fortunately, the considered complicated system can be solved analytically and therefore, we will be able to evaluate the time evolution of some of the physical properties such as atomic inversion and entropy squeezing. Since the exact solution depends on the initial atom–field state, we will take the atom to be in its exited state, and the field is considered to be in a coherent state, a squeezed state and a thermal state. Although, our proposal may work well for any arbitrary nonlinear physical system with known $f(n)$, the effect of various parameters and different initial field states will be investigated in detail by considering a particular nonlinearity function.

The paper is organized in the following way. In Section 2, we introduce the interaction Hamiltonian of our considered system in the full nonlinear regime of k-photon JCM, and then by solving the corresponding Schrödinger equation, the probability amplitudes at any time t for the whole system with arbitrary initial field state are obtained. In Sections 3 and 4, we investigate the temporal evolution of atomic inversion and entropy squeezing, respectively. Section 5 presents our numerical results for atomic inversion and entropy squeezing corresponding to single- and two-photon transitions. In detail, we discuss the effects of the Kerr medium, the Stark shift, detuning and intensity-dependent coupling on the evolution of the mentioned physical quantities. As we continue, the results of the effects of three- and four-photon transitions on the time evolution of atomic inversion and entropy squeezing are briefly given in Section 6. Finally, we give a summary and conclusions in Section 7.

2. The k-photon JCM: full nonlinear regime

The Hamiltonian of a two-level atom interacting with a quantized field in the standard JCM in the dipole and the rotating wave approximations can be simply written as ($\hbar = 1$), $\hat{H} = \nu\hat{a}^{\dagger}\hat{a} + \omega\hat{\sigma}_z/2 + \lambda(\hat{a}^{\dagger}\hat{\sigma}_- + \hat{a}\hat{\sigma}_+)$, where $\hat{\sigma}_z$ and $\hat{\sigma}_{\pm}$ are the Pauli operators, $\hat{a}$ and $\hat{a}^{\dagger}$ are the bosonic annihilation and creation operators, respectively, ν is the frequency of the field, ω is the transition frequency between the excited and the ground states of the atom, and λ is the coupling constant. By generalizing the standard JCM over a few steps, the time-dependent single-mode k-photon JCM in the presence of a linear Stark shift and a Kerr medium with the time-dependent coupling can be described by the Hamiltonian[34]

$$\begin{aligned}\hat{H}(t) &= \nu\hat{a}^{\dagger}\hat{a} + \frac{\omega}{2}\hat{\sigma}_z + \hat{a}^{\dagger}\hat{a}(\beta_1|g\rangle\langle g| + \beta_2|e\rangle\langle e|) \\ &\quad + \chi\hat{a}^{\dagger 2}\hat{a}^2 + \lambda(t)(\hat{a}^{\dagger k}\hat{\sigma}_- + \hat{a}^k\hat{\sigma}_+), \end{aligned} \tag{1}$$

where β_1 and β_2 are the effective Stark coefficients, χ denotes the third-order susceptibility of the Kerr medium and $\lambda(t)$ is the time-dependent coupling parameter. The third term in Hamiltonian (1) indicates the linear (in $a^{\dagger}a$) Stark shift effect, which arises from the virtual transition to the intermediate level,[35–37] and can exist for a two-photon transition, i.e., $k = 2$.[35] So, for instance, the authors of Refs. [34] and [38] used $\delta_{k,2}$ besides the Stark shift term in their Hamiltonian. In addition, it should be emphasized that, in Hamiltonian (1), whenever $k \neq 2$, one has to set $\beta_1 = 0 = \beta_2$.[38] It is worth mentioning that the (nonlinear) Stark shift can also exist for the cases with $k > 2$.[36] In this latter case, Hamiltonian (1) changes to the following form:

$$\begin{aligned}\hat{H}(t) &= \nu\hat{a}^{\dagger}\hat{a} + \frac{\omega}{2}\hat{\sigma}_z + \hat{a}^{\dagger k}\hat{a}^k(\beta_1|g\rangle\langle g| + \beta_2|e\rangle\langle e|) \\ &\quad + \chi\hat{a}^{\dagger 2}\hat{a}^2 + \lambda(t)(\hat{a}^{\dagger 2k}\hat{\sigma}_- + \hat{a}^{2k}\hat{\sigma}_+). \end{aligned} \tag{2}$$

Hamiltonian (2) for $k = 1$ is equal to Hamiltonian (1) for $k = 2$ (the linear Stark shift can occur). In this paper, following the path in Ref. [34], we will generalize Hamiltonian (1), which is performed for the linear Stark shift effect, in order to be able

to compare our results with the results in Ref. [34]. By defining the detuning parameter $\Delta = \omega - k\nu$, Hamiltonian (1) can be rewritten in the form

$$\hat{H}(t) = \nu\left(\hat{a}^{\dagger}\hat{a} + \frac{k}{2}\hat{\sigma}_z\right) + \frac{\Delta}{2}\hat{\sigma}_z + \hat{a}^{\dagger}\hat{a}(\beta_1|g\rangle\langle g| + \beta_2|e\rangle\langle e|) + \chi\hat{a}^{\dagger 2}\hat{a}^2 + \lambda(t)(\hat{a}^{\dagger k}\hat{\sigma}_- + \hat{a}^k\hat{\sigma}_+). \quad (3)$$

The aim of this paper is to generalize all terms of Hamiltonian (3) via the well-known nonlinear coherent state approach.[39,40] By the notion of nonlinearity we mean that we intend to put the f-deformation function in all possible terms, i.e., we will replace all $\hat{a}$ and $\hat{a}^{\dagger}$ respectively by $\hat{A} = \hat{a}f(\hat{n})$ and $\hat{A}^{\dagger} = f(\hat{n})\hat{a}^{\dagger}$, where $f(\hat{n})$ is a function of the number operator (intensity of light). By performing the mentioned procedure, the full nonlinear single-mode k-photon time-dependent JCM in the presence of an effective Stark shift and a Kerr medium can be written in the following manner:

$$\hat{H}(t) = \nu\left(\hat{A}^{\dagger}\hat{A} + \frac{k}{2}\hat{\sigma}_z\right) + \frac{\Delta}{2}\hat{\sigma}_z + \hat{A}^{\dagger}\hat{A}(\beta_1|g\rangle\langle g| + \beta_2|e\rangle\langle e|) + \chi\hat{A}^{\dagger 2}\hat{A}^2 + \lambda(t)(\hat{A}^{\dagger k}\hat{\sigma}_- + \hat{A}^k\hat{\sigma}_+). \quad (4)$$

In this respect, a few words seem to be necessary about our present work. It may be recognized that, starting with the nonlinear Hamiltonian describing the interaction between a three-level atom and a single-mode f-deformed cavity field (without the Stark shift) and following the path of Refs. [35] and [36], the same equations of motion for the three levels of the atom will be achieved. Therefore, one can conclude that, replacing $a, a^{\dagger}$ with $A, A^{\dagger}$ does not change the final results. However we would like to emphasize that the Stark shift should exist in the generalized form of Hamiltonian (4), too. In other words, the Stark shift coefficients are now linear in terms of $\hat{A}^{\dagger}\hat{A}$, i.e., the field part of Hamiltonian (4). So, in Hamiltonian (4) (similar to Hamiltonians (1) and (3)), the linear (in terms of $\hat{A}^{\dagger}\hat{A}$) Stark shift can exist for the case of $k = 2$. Whenever $k \neq 2$ one should set $\beta_1 = 0 = \beta_2$. To see what we have really done explicitly, we put

$$\hat{H}(t) = \nu\left(\hat{a}^{\dagger}\hat{a}f^2(\hat{n}) + \frac{k}{2}\hat{\sigma}_z\right) + \frac{\Delta}{2}\hat{\sigma}_z + \hat{a}^{\dagger}\hat{a}f^2(\hat{n})(\beta_1|g\rangle\langle g| + \beta_2|e\rangle\langle e|) + \chi f^2(\hat{n})f^2(\hat{n}-1)\hat{a}^{\dagger 2}\hat{a}^2 + \lambda(t)\left(\frac{[f(\hat{n})]!}{[f(\hat{n}-k)]!}\hat{a}^{\dagger k}\hat{\sigma}_- + \hat{a}^k\frac{[f(\hat{n})]!}{[f(\hat{n}-k)]!}\hat{\sigma}_+\right), \quad (5)$$

where $\hat{n} = \hat{a}^{\dagger}\hat{a}$ and $[f(\hat{n})]! \doteq f(\hat{n})f(\hat{n}-1)\cdots f(1)$ with $[f(0)]! \doteq 1$. By comparing Hamiltonian (6) with previous Hamiltonian (3), which was considered in Ref. [34], it is clear that we have in fact made the transformations $\nu \to \nu f^2(\hat{n})$, $\beta_{1(2)} \to \beta_{1(2)}f^2(\hat{n})$, $\chi \to \chi f^2(\hat{n})f^2(\hat{n}-1)$ and $\lambda(t) \to \lambda(t)[f(\hat{n}]!/[f(\hat{n}-k)]!$. It is seen that the field frequency, Stark shifts, the third-order susceptibility and the time-dependent parameter are all evolved from c numbers to operator-valued functions (intensity-dependent parameters).[22,23,29,39,41]

The time-dependent λ parameter makes the whole Hamiltonian be time-dependent. Different forms may be chosen for $\lambda(t)$. In this paper, we will select $\lambda(t) = \gamma\cos(\mu t)$, where γ and μ are arbitrary constants. Following the probability amplitude approach,[3] we assume that the wave function of the atom–field can be expressed as[42]

$$|\psi(t)\rangle = \sum_n \exp[-i\nu(\hat{n}f^2(\hat{n}) + k\hat{\sigma}_z/2)](c_{n,e}(t)|n,e\rangle + c_{n+k,g}(t)|n+k,g\rangle), \quad (6)$$

where $|n,e\rangle$ and $|n+k,g\rangle$ are the states in which the atom is in the exited and the ground states and the field has n and $n+k$ photons, respectively. Substituting wave function (6) in the time-dependent Schrödinger equation, $i\hbar(\partial/\partial t)|\psi(t)\rangle = \hat{H}|\psi(t)\rangle$, we obtain the following coupled equations for $c_{n,e}(t)$ and $c_{n+k,g}(t)$:

$$i\frac{dc_{n,e}}{dt} = R_1 c_{n,e}(t) + \alpha_n\cos(\mu t)c_{n+k,g}(t),$$
$$i\frac{dc_{n+k,g}}{dt} = R_2 c_{n+k,g}(t) + \alpha_n\cos(\mu t)c_{n,e}(t), \quad (7)$$

where R_1, R_2 and α_n are defined as

$$R_1 = \frac{\Delta}{2} + nf^2(n)\beta_2 + \chi n(n-1)f^2(n)f^2(n-1),$$
$$R_2 = -\frac{\Delta}{2} + (n+k)f^2(n+k)\beta_1 + \chi(n+k)(n+k-1)f^2(n+k)f^2(n+k-1),$$
$$\alpha_n = \gamma\frac{[f(n+k)]!}{[f(n)]!}\sqrt{\frac{(n+k)!}{n!}}. \quad (8)$$

The fast frequency dependence of $c_{n,e}(t)$ and $c_{n+k,g}(t)$ can be removed by transforming them to the slowly varying functions $X(t)$ and $Y(t)$ as

$$X(t) = c_{n,e}(t)\exp(iR_1 t), \quad Y(t) = c_{n+k,g}(t)\exp(iR_2 t). \quad (9)$$

Using Eq. (9) in Eq. (7), we obtain

$$\frac{dX}{dt} = -i\frac{\alpha_n}{2}(e^{i(\mu+R_n)t} + e^{-i(\mu-R_n)t})Y,$$
$$\frac{dY}{dt} = -i\frac{\alpha_n}{2}(e^{i(\mu-R_n)t} + e^{-i(\mu+R_n)t})X, \quad (10)$$

where

$$R_n = R_1 - R_2 = \Delta + \chi[n(n-1)f^2(n)f^2(n-1) - (n+k)(n+k-1)f^2(n+k)f^2(n+k-1)] + [nf^2(n)\beta_2 - (n+k)f^2(n+k)\beta_1]. \quad (11)$$

The coupled differential equations (10) consist of two terms; the term in the form $e^{i(\mu-R_n)t}$ ($e^{i(\mu+R_n)t}$) describes the process in which the energy is conserved (nonconserved). We

neglect the energy nonconserving terms (in the rotating wave approximation). Under this condition, equations (10) change to

$$\begin{aligned}\frac{\mathrm{d}X}{\mathrm{d}t} &= -\mathrm{i}\frac{\alpha_n}{2}\mathrm{e}^{-\mathrm{i}(\mu-R_n)t}Y,\\ \frac{\mathrm{d}Y}{\mathrm{d}t} &= -\mathrm{i}\frac{\alpha_n}{2}\mathrm{e}^{\mathrm{i}(\mu-R_n)t}X.\end{aligned} \tag{12}$$

By solving the above coupling equations, we obtain

$$\begin{aligned}c_{n,e}(t) &= \left\{c_{n,e}(0)\left(\cos(\Omega_n t)-\mathrm{i}(R_n-\mu)\frac{\sin(\Omega_n t)}{2\Omega_n}\right)\right.\\ &\quad\left.-\mathrm{i}\frac{\alpha_n}{2\Omega_n}\sin(\Omega_n t)c_{n+k,g}(0)\right\}\\ &\quad\times\exp[-\mathrm{i}(\varphi_n+\mu/2)t],\end{aligned} \tag{13}$$

$$\begin{aligned}c_{n+k,g}(t) &= \left\{c_{n+k,g}(0)\left(\cos(\Omega_n t)+\mathrm{i}(R_n-\mu)\frac{\sin(\Omega_n t)}{2\Omega_n}\right)\right.\\ &\quad\left.-\mathrm{i}\frac{\alpha_n}{2\Omega_n}\sin(\Omega_n t)c_{n,e}(0)\right\}\\ &\quad\times\exp[-\mathrm{i}(\varphi_n-\mu/2)t],\end{aligned} \tag{14}$$

where

$$\begin{aligned}\varphi_n &= \frac{\chi}{2}[n(n-1)f^2(n)f^2(n-1)\\ &\quad+(n+k)(n+k-1)f^2(n+k)f^2(n+k-1)]\\ &\quad+\frac{1}{2}[nf^2(n)\beta_2+(n+k)f^2(n+k)\beta_1].\end{aligned} \tag{15}$$

Here $\Omega_n=\sqrt{(R_n-\mu)^2+\alpha_n^2}/2$ is the generalized Rabi frequency (note that α_n and R_n are defined respectively in Eqs. (8) and (11)). It ought to be mentioned that in Eqs. (8), (11) and (15), $\beta_1=0=\beta_2$ should be set for the case of $k\neq 2$.

In the above equations, $c_{n,e}(0)$ and $c_{n+k,g}(0)$ may be determined with the initial states of the atom and the field. In this work, we suppose that the atom is initially in the excited state $|e\rangle$, and the cavity field is considered to be initially in different states such as a coherent state, a squeezed state and a thermal state, which can be defined by their associated density operators as

$$\rho_{\mathrm{CS}}(0)=|\alpha\rangle\langle\alpha|=\mathrm{e}^{-\langle n\rangle}\sum_{n,m=0}^{\infty}\frac{\alpha^m\alpha^{*n}}{\sqrt{m!n!}}|m\rangle\langle n|, \tag{16}$$

$$\begin{aligned}\rho_{\mathrm{SS}}(0) &= |\xi\rangle\langle\xi|\\ &= \sum_{n,m=0}^{\infty}\frac{(\tanh r)^{n+m}\sqrt{(2m)!(2n)!}}{(2^n n!2^m m!)\cosh r}|2m\rangle\langle 2n|,\end{aligned} \tag{17}$$

$$\rho_{\mathrm{TS}}(0)=\sum_{n=0}^{\infty}\frac{\langle n\rangle^n}{(1+\langle n\rangle)^{n+1}}|n\rangle\langle n|. \tag{18}$$

Therefore, by using each of the above initial field conditions, we can find the explicit form of the solution of the time-dependent Schrödinger equation. This enables us to analyze interesting properties such as atomic inversion and entropy squeezing, which will be done in the following sections.

It can be seen clearly that setting $f(n)=1$ in relations (13) and (14) recovers the results in Ref. [34]. Another important point worth mentioning is that choosing different nonlinearity functions leads to different Hamiltonian systems and so, different physical results may be obtained. In the rest of this paper, we particularly select the intensity-dependent coupling as $f(n)=\sqrt{n}$. This function is a favorite function for the authors who have worked in the nonlinear regime of the atom–field interaction (see for instance Refs. [41] and [43]). In particular, Fink *et al.* have shown in a natural way that this nonlinearity function can appear in physical systems.[44]

3. Atomic inversion

The atomic inversion measures the difference in the populations of the two levels of the atom and plays a fundamental role in the laser theory.[42] After determining $c_{n,e}(t)$ and $c_{n+k,g}(t)$ for the initial field states in Eqs. (16)–(18), we can investigate the quantity

$$W(t)=\sum_{n=0}^{\infty}(|c_{n,e}(t)|^2-|c_{n+k,g}(t)|^2). \tag{19}$$

By inserting Eqs. (13) and (14) in Eq. (19) for an arbitrary initial field state, we obtain

$$W(t)=\sum_{n=0}^{\infty}\rho_{nn}(0)\left(\cos(2\Omega_n t)+(R_n-\mu)^2\frac{\sin^2(\Omega_n t)}{2\Omega_n^2}\right), \tag{20}$$

where $\rho_{nn}(0)=|c_n(0)|^2$. For the mentioned initial field states in Eqs. (16)–(18), we have

$$\rho_{n,n}^{\mathrm{CS}}(0)=|c_n^{\mathrm{CS}}(0)|^2=\mathrm{e}^{-\langle n\rangle}\frac{\langle n\rangle^{2n}}{n!}, \tag{21}$$

$$\rho_{2n,2n}^{\mathrm{SS}}(0)=|c_{2n}^{\mathrm{SS}}(0)|^2=\frac{\langle n\rangle^n(2n)!}{(2^n n!)^2(1+\langle n\rangle)^{n+1/2}},$$

$$\rho_{2n+1,2n+1}^{\mathrm{SS}}(0)=|c_{2n+1}^{\mathrm{SS}}(0)|^2=0, \tag{22}$$

$$\rho_{n,n}^{\mathrm{TS}}(0)=\frac{\langle n\rangle^n}{(1+\langle n\rangle)^{n+1}}, \tag{23}$$

where $\langle n\rangle$ of these states are given by

$$\langle n\rangle_{\mathrm{CS}}=|\alpha|^2,\ \ \langle n\rangle_{\mathrm{SS}}=\sinh^2(r),\ \ \langle n\rangle_{\mathrm{TS}}=\frac{1}{\mathrm{e}^{\hbar\nu/k_{\mathrm{B}}T}-1}. \tag{24}$$

From Eq. (20), we can discuss the temporal evolution of the atomic inversion for different initial field situations. This will be presented in Section 5 in detail.

4. Entropy squeezing

For a two-level atom, characterized by the Pauli operators σ_x, σ_y, and σ_z, the uncertainty relation for the information entropy is defined as follows:[11]

$$\delta H(\sigma_x)\delta H(\sigma_y)\geq\frac{4}{\delta H(\sigma_z)},\ \ \delta H(\sigma_\alpha)=\exp[H(\sigma_\alpha)], \tag{25}$$

where $H(\sigma_\alpha)$, as the information entropy of operator σ_α ($\alpha = x,y,z$), is given by

$$H(\sigma_\alpha) = -\sum_{i=1}^{2} P_i(\sigma_\alpha)\ln P_i(\sigma_\alpha). \tag{26}$$

Since for a two-level atom, the Pauli operators have two eigenvalues, one may expect that $P_i(\sigma_\alpha)$ denotes the probability distribution of two possible outcomes of the measurements of operator σ_α. Henceforth, it is defined as

$$P_i(\sigma_\alpha) = \langle\psi_{\alpha_i}|\rho|\psi_{\alpha_i}\rangle, \tag{27}$$

where ρ is the density operator of the system and $|\psi_{\alpha_i}\rangle$ is the eigenstate of the Pauli operators, i.e.,

$$\sigma_\alpha|\psi_{\alpha_i}\rangle = \eta_{\alpha_i}|\psi_{\alpha_i}\rangle, \quad \alpha = x,y,z, \quad i = 1,2. \tag{28}$$

From Eq. (25), the component σ_α ($\alpha = x,y$) is said to be squeezed if the information entropy $H(\sigma_\alpha)$ of σ_α satisfies the inequality

$$E(\sigma_\alpha) = \delta H(\sigma_\alpha) - \frac{2}{\sqrt{\delta H(\sigma_z)}} < 0, \quad \alpha = x \text{ or } y. \tag{29}$$

By using Eqs. (26) and (27) for the information entropies of the atomic operators σ_x, σ_y, and σ_z, we finally arrive at

$$\begin{aligned} H(\sigma_x) &= -\left[\frac{1}{2}+\mathrm{Re}(\rho_{ge}(t))\right]\ln\left[\frac{1}{2}+\mathrm{Re}(\rho_{ge}(t))\right] \\ &\quad -\left[\frac{1}{2}-\mathrm{Re}(\rho_{ge}(t))\right]\ln\left[\frac{1}{2}-\mathrm{Re}(\rho_{ge}(t))\right], \end{aligned} \tag{30}$$

$$\begin{aligned} H(\sigma_y) &= -\left[\frac{1}{2}+\mathrm{Im}(\rho_{ge}(t))\right]\ln\left[\frac{1}{2}+\mathrm{Im}(\rho_{ge}(t))\right] \\ &\quad -\left[\frac{1}{2}-\mathrm{Im}(\rho_{ge}(t))\right]\ln\left[\frac{1}{2}-\mathrm{Im}(\rho_{ge}(t))\right], \end{aligned} \tag{31}$$

$$H(\sigma_z) = -\rho_{ee}(t)\ln\rho_{ee}(t) - \rho_{gg}(t)\ln\rho_{gg}(t). \tag{32}$$

By using the form of wave function (6), the density operator of the entire atom–field system at any time t is given by

$$\begin{aligned} \rho_{\text{atom-field}} = \sum_{n=0}^{\infty}\sum_{m=0}^{\infty} &\{c_{n,e}(t)c^*_{m,e}(t)|n,e\rangle\langle e,m| \\ &+ c_{n+k,g}(t)c^*_{m+k,g}(t)|n+k,g\rangle\langle g,m+k| \\ &+ c_{n,e}(t)c^*_{m+k,g}(t)|n,e\rangle\langle g,m+k| \\ &+ c_{n+k,g}(t)c^*_{m,e}(t)|n+k,g\rangle\langle e,m|\}. \end{aligned} \tag{33}$$

So the necessary matrix elements of the reduced density operator in Eqs. (30)–(32) may be given in the following form:

$$\rho_{ee}(t) = \sum_{n=0}^{\infty}|c_{n,e}(t)|^2, \tag{34}$$

$$\rho_{eg}(t) = \sum_{n=0}^{\infty} c_{n+k,e}(t)c^*_{n+k,g}(t) = \rho^*_{ge}(t), \tag{35}$$

$$\rho_{gg}(t) = \sum_{n=0}^{\infty}|c_{n+k,g}(t)|^2. \tag{36}$$

By employing the above equations, we can study the temporal evolution of the entropy squeezing in terms of variables σ_x and σ_y, which will be done in the next section.

5. Results and discussion

By using Eq. (20) and replacing $\rho_{nn}(0)$ with different initial field states (the coherent, squeezed and thermal states from Eqs. (21)–(23)), we can investigate the effects of the initial field state on the variation of the atomic inversion. Now it is necessary to select a particular nonlinearity function. As we mentioned previously, we have chosen $f(n) = \sqrt{n}$ in this paper. In all figures that are related to the atomic inversion $W(t)$, the left and the right plots correspond to the linear and the nonlinear functions, respectively. All figures are drawn with particular values of $\mu = 0.1$ and $\langle n\rangle = 25$. The other parameters used are denoted in the figure captions.

Figure 1 shows the temporal evolution of the atomic inversion in terms of the scaled time, for the functions $f(n) = \sqrt{n}$ and $f(n) = 1$, taking the coherent state in Eq. (16) as the initial field state. Figures 1(a) and 1(b) show the variation of the atomic inversion without Kerr and Stark effects. The collapse and revival phenomena are observed in these figures, and there is an increase in fluctuation for the deformed case compared with the regular behavior. The amplitude of the fluctuation for this case is increased relative to that with $f(n) = 1$. In other words, while we have partial revivals in the linear case, nearly complete revivals occur in the nonlinear regime. To examine the effect of the Kerr medium on the behavior of the population inversion, figures 1(c) and 1(d) are plotted. Figure 1(d), which corresponds to $f(n) = \sqrt{n}$, shows a chaotic behavior of $W(t)$ around 0.99, and the amplitude of the fluctuations between the maxima and minima of $W(t)$ is very small. Figure 1(c) indicates that in the presence of the Kerr effect for the case of $f(n) = 1$, the result is very similar to that in Fig. 1(a). If we use a larger χ (up to 0.03[34]), the Kerr effect will be visible. The effect of the Stark shift (in the presence of the Kerr medium) can be seen for linear and nonlinear functions in Figs. 1(e) and 1(f). From Fig. 1(f), we observe that the Stark shift increases the amplitude of the fluctuation as compared with that in Fig. 1(d). This figure also shows a chaotic behavior for $W(t)$ in the nonlinear regime. Figure 1(e) shows the effect of the Stark shift (in the presence of the Kerr medium) on the time variation of $W(t)$ for $f(n) = 1$. One can see that the temporal evolution of the atomic inversion reveals several revivals in the presence of both the Stark and the Kerr effects.

Comparing Figs. 1(e) and 1(b) leads us to a conclude that the effect of the considered nonlinearity function (without the Kerr and the Stark effects) is nearly equivalent to the Kerr and the Stark effects in the linear case.

The effect of the detuning parameter Δ (defined as $\omega - k\nu = \Delta$), in the presence of the Kerr and the Stark effects, is shown in Figs. 1(g) and 1(h). Comparing Fig. 1(g) with Fig. 1(e), we find that the extremes of $W(t)$ (in the revivals) are regularly decreased for the linear system. The Δ has a negligible effect in the presence of a nonlinearity function (Fig. 1(h)).

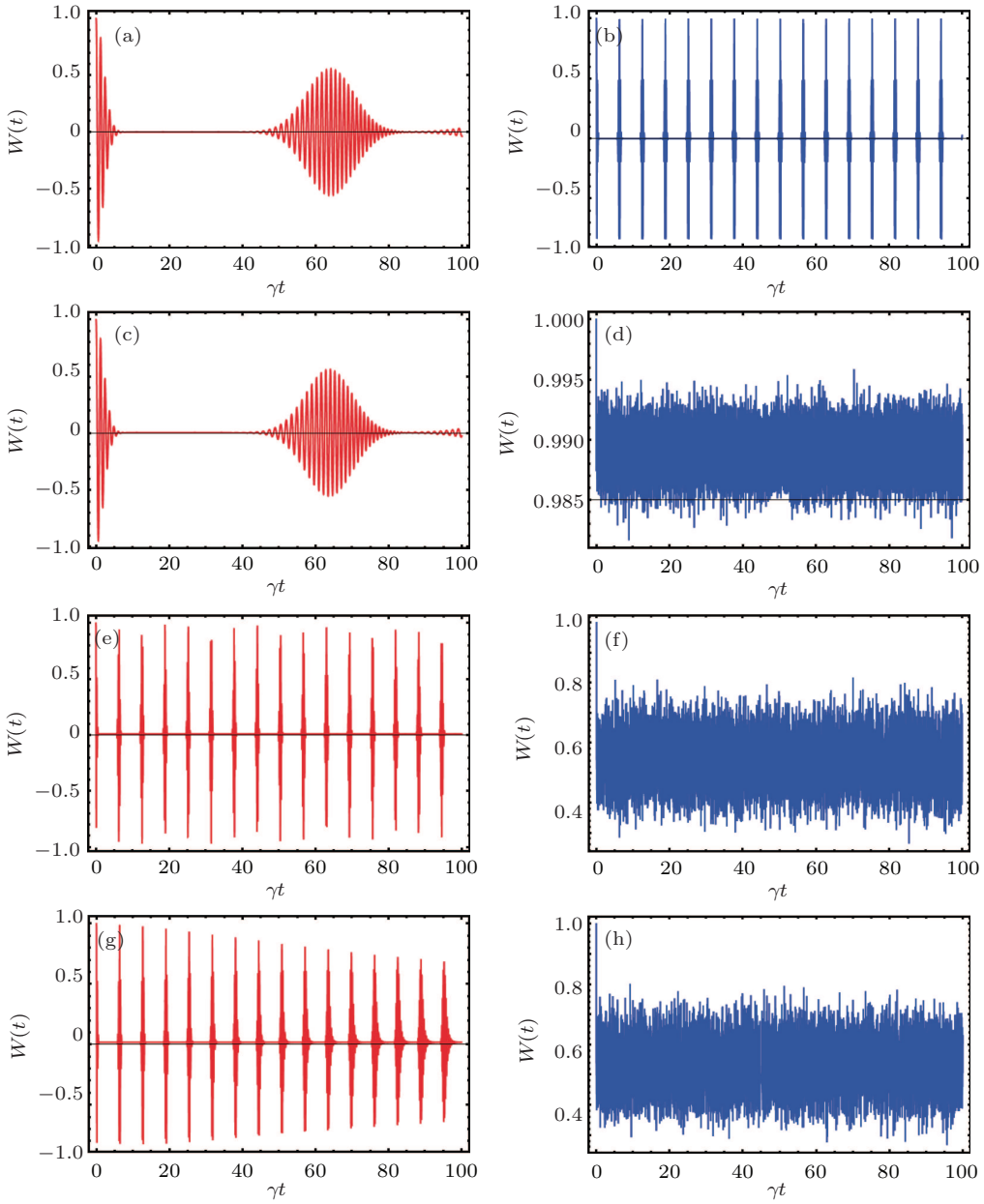


Fig. 1. (color online) Evolution of atomic inversion versus scaled time γt, here the atom starts in the exited state and the field in a coherent state with $\langle n\rangle = 25, \mu = 0.1$: (a) $f(n) = 1, \Delta = 0, \chi = 0, k = 1, \beta_1 = \beta_2 = 0$; (b) $f(n) = \sqrt{n}, \Delta = 0, \chi = 0, k = 1, \beta_1 = \beta_2 = 0$; (c) $f(n) = 1, \Delta = 0, \chi = 0.005, k = 1, \beta_1 = \beta_2 = 0$; (d) $f(n) = \sqrt{n}, \Delta = 0, \chi = 0.005, k = 1, \beta_1 = \beta_2 = 0$; (e) $f(n) = 1, \Delta = 0, \chi = 0.005, k = 2, \beta_1 = \beta_2 = 1$; (f) $f(n) = \sqrt{n}, \Delta = 0, \chi = 0.005, k = 2, \beta_1 = \beta_2 = 1$; (g) $f(n) = 1, \Delta = 6, \chi = 0.005, k = 2, \beta_1 = \beta_2 = 1$; (h) $f(n) = \sqrt{n}, \Delta = 6, \chi = 0.005, k = 2, \beta_1 = \beta_2 = 1$.

We plot Fig. 2 by taking into account the initial field as the squeezed state in Eq. (17). Figures 2(a) and 2(b) show the time evolutions of the atomic inversion for the linear and the nonlinear functions in the absence of both Kerr and Stark effects. We can see from Fig. 2(a) that $W(t)$ oscillates rapidly for the case of $f(n) = 1$, while in the presence of nonlinearity, the behavior of $W(t)$ is periodic (Fig. 2(b)). Figures 2(c) and 2(d) demonstrate the effect of the Kerr medium on the variation of $W(t)$; and in Figs. 2(e) and 2(f), we add the Stark shift too. By comparing Figs. 2(a) and 2(c), we find that the behaviors of $W(t)$ for $f(n) = 1$ with and without the Kerr effect are almost the same. However, for the linear case and in the presence of the Stark effect (Fig. 2(e)), the behavior of $W(t)$ is irregular. We examine the time evolution of the atomic inversion for the nonlinear case with different parameters in the right panels of Fig. 2. We can find a regular behavior for $W(t)$ in the absence of the Kerr medium, the Stark effect and detuning (Fig. 2(b)). The behaviors of $W(t)$ in Figs. 2(d), 2(f), and 2(h) are generally irregular.

In Fig. 3, we assume that the initial field is the thermal state in Eq. (18), and again the effects of the Kerr medium, the Stark shift and detuning are investigated on the behavior of $W(t)$. The evolution of the atomic inversion is shown for the nonlinear and linear regimes in the right and the left panels of the

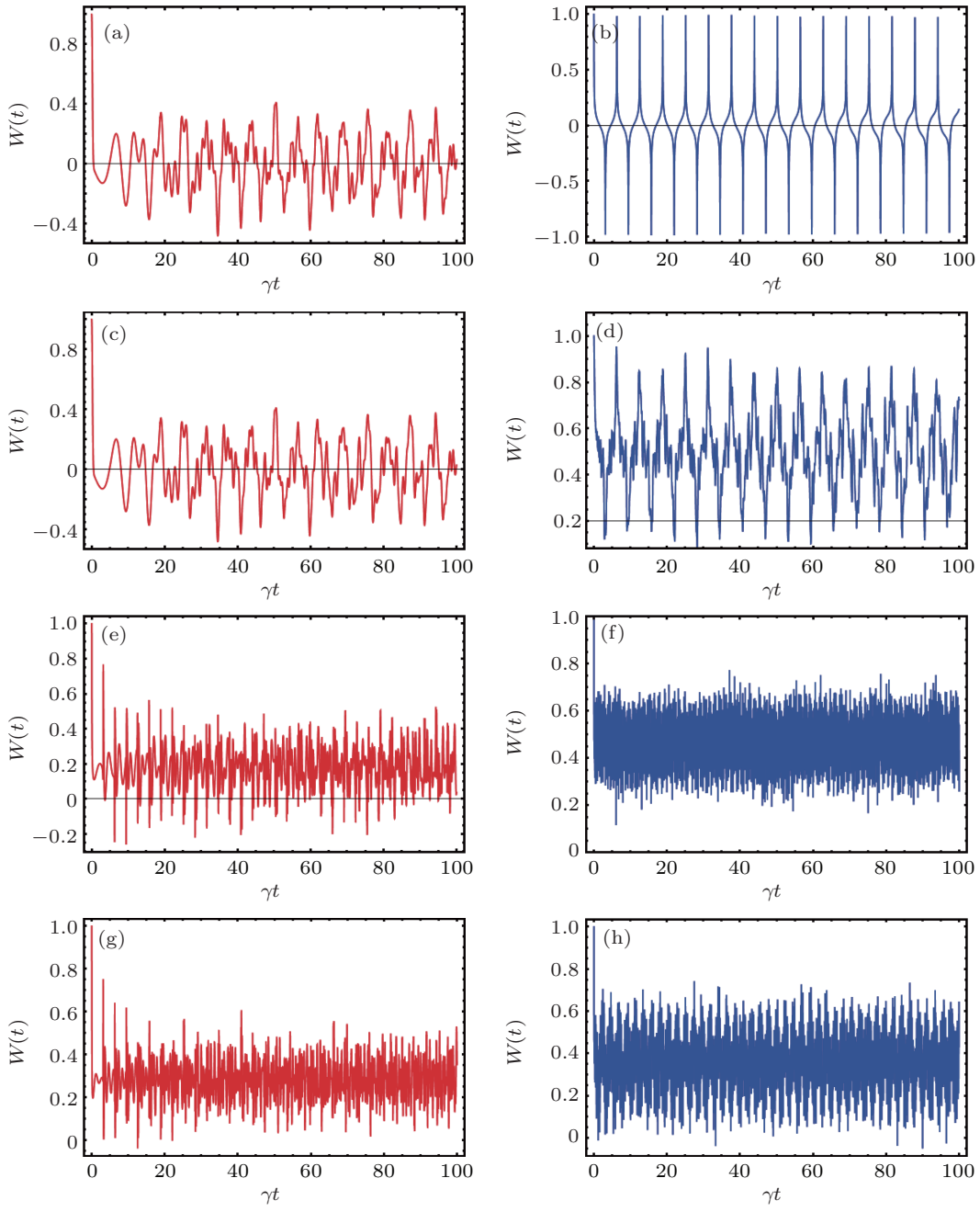


Fig. 2. (color online) Evolution of atomic inversion versus scaled time γt, where a squeezed state is used as the initial state of the field. The parameters used in panels (a)–(h) are the same as those in Fig. 1.

figure, respectively. The effect of the Kerr medium is shown in Fig. 3(c) for the linear function, where we can see that $W(t)$ is not so sensitive to the Kerr effect. While in Fig. 3(b), the presence of nonlinearity without both Kerr and Stark effects allows the (partial) collapses and revivals to be observed, the Kerr medium and the Stark shift destroy the latter phenomena. The above result seems to be in contrast to that in the linear case, i.e., the presence of Kerr and Stark shift effects can lead to the (partial) collapses and revivals.

We show the variations of $W(t)$ with $\Delta \neq 0$ in the presence of the Kerr and the Stark effects for linear and nonlinear functions in Figs. 3(g) and 3(h), respectively. Unlike some changes in the numerical results, no qualitatively change can be observed. Generally, in all the three states discussed above, the linear case is more sensitive to detuning in comparison with the nonlinear case.

We now analyze the temporal evolution of the entropy squeezing for different initial field states using the analytical results of Section 4. We will deal with the nonlinear case with deformation function $f(n) = \sqrt{n}$ only. All figures are drawn with a particular value of $\mu = 0.1$. The other parameters used are denoted in the figure captions. Figures 4(a) and 4(b) display the time evolutions of the entropy squeezing factors $E(\sigma_x)$ and $E(\sigma_y)$ with the coherent state in Eq. (18) as the initial field state. It is obvious from these figures that entropy squeezing exists in σ_x and σ_y at some time.

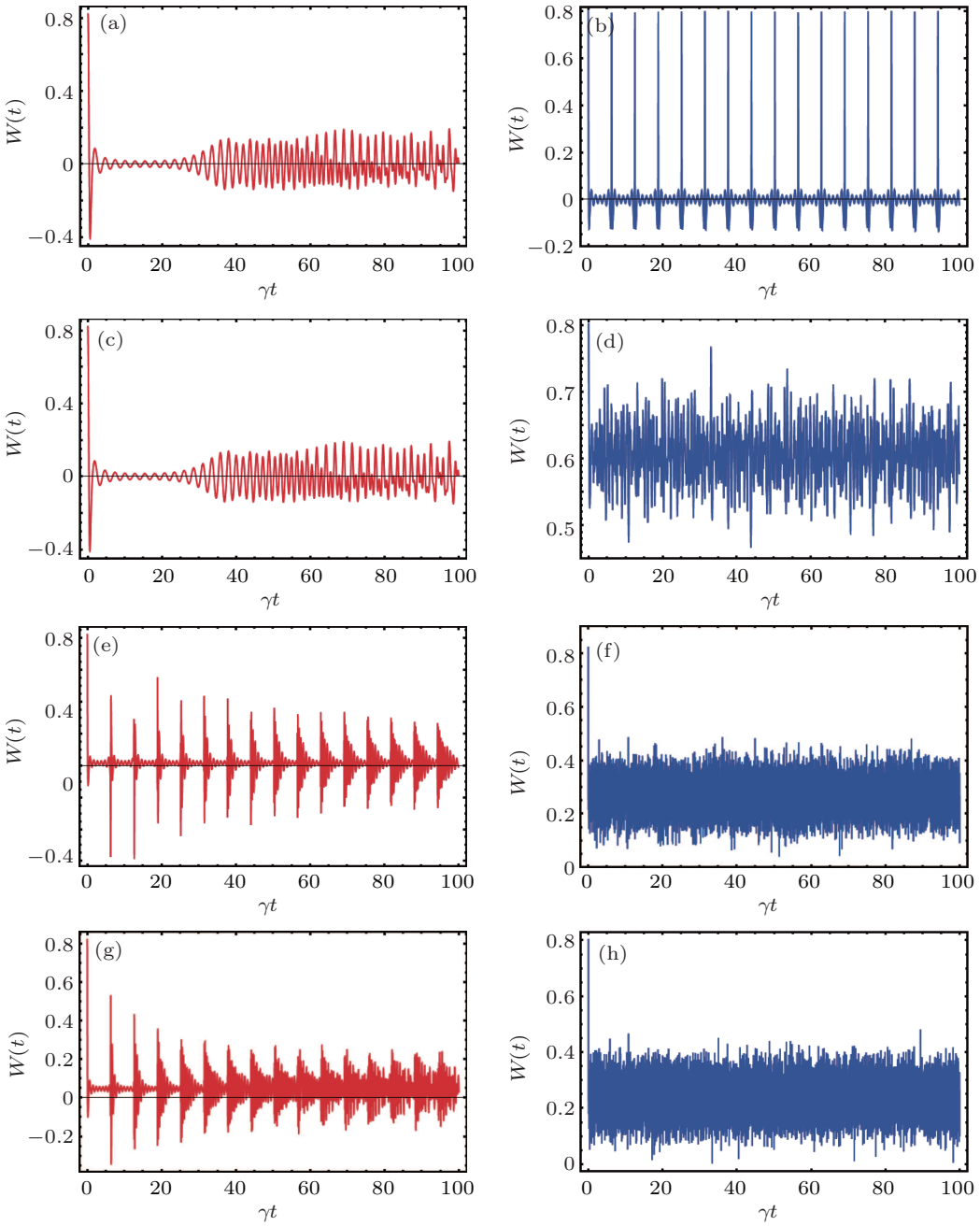


Fig. 3. (color online) Evolution of atomic inversion versus scaled time γt, where a thermal state is used as the initial state of the field. The parameters used in panels (a)–(h) are the same as those in Fig. 1.

In Figs. 4(c) and 4(d), we examine the influence of the Kerr effect on the evolution of the entropy squeezing for variables σ_x and σ_y with the chosen parameters. It is clear from these figures that there is no squeezing in σ_x and σ_y. In Figs. 4(e) and 4(f), which are plotted in the presence of both Kerr and Stark effects, no squeezing can be seen in σ_x and σ_y. To study the effect of the initial mean photon number on the behavior of the entropy squeezing (with the Kerr effect), figures 4(g) and 4(h) are plotted.

As is shown, by decreasing the mean value of $\langle n \rangle$ from 25 to 1, the entropy squeezing for variables σ_x and σ_y appears in certain time ranges. The time evolution of the squeezing parameters $E(\sigma_x)$ and $E(\sigma_y)$ are shown in Fig. 5 with the field initially g in the squeezed state (19).

Specifically, in Figs. 5(a) and 5(b), the behaviors of squeezing $E(\sigma_x)$ and $E(\sigma_y)$ as a function of the scaled time in the absence of the Kerr and the Stark effects are shown. We can see from these figures that both $E(\sigma_x)$ and $E(\sigma_y)$ possess squeezing in variables σ_x and σ_y when $\langle n \rangle = 1$. It should be noticed that according to our further calculations (not shown here), in this case (without Kerr and Stark effects), squeezing may be seen in components σ_x and σ_y for $\langle n \rangle < 4$. To investigate the effect of the Kerr medium, we depict the entropy squeezing $E(\sigma_x)$ and $E(\sigma_y)$ in terms of the scaled time in Figs. 5(c) and 5(d). The $E(\sigma_x)$ and $E(\sigma_y)$ predict squeezing in variables σ_x and σ_y on short time periods discontinuously. A

comparison of Figs. 5(a)–5(d) with similar figures for the coherent state (Figs. 4(a)–4(d)) shows that, while for the second set of figures the Kerr effect destroys the entropy squeezing completely, this is not the case for the first set of figures. We show the effects of the Stark shift on the time evolutions of the squeezing factors in Figs. 5(e) and 5(f). It is obvious from these figures that, there is no squeezing in the presence of the Kerr and the Stark effects. Figure 6 shows the time evolutions of the entropy squeezing factors $E(\sigma_x)$ and $E(\sigma_y)$ for the case in which the field is initially prepared in the thermal state (18). Figures 6(a) and 6(b) present the entropy squeezing $E(\sigma_x)$ and $E(\sigma_y)$ in the absence of the Kerr and the Stark effects. As is clearly seen, squeezing in components σ_x and σ_y exists at some intervals of time, and obviously for different time intervals. The depth of the entropy squeezing for σ_x is larger than that for σ_y. We investigate the effect of the Kerr medium in Figs. 6(c) and 6(d). As is observed, squeezing may occur in entropy squeezing factors $E(\sigma_x)$ and $E(\sigma_y)$ over a short range of time. Finally, we examine the effect of the Stark shift (the Kerr effect is also included) in Figs. 6(e) and 6(f). In this case, there is no squeezing in $E(\sigma_x)$ and $E(\sigma_y)$.

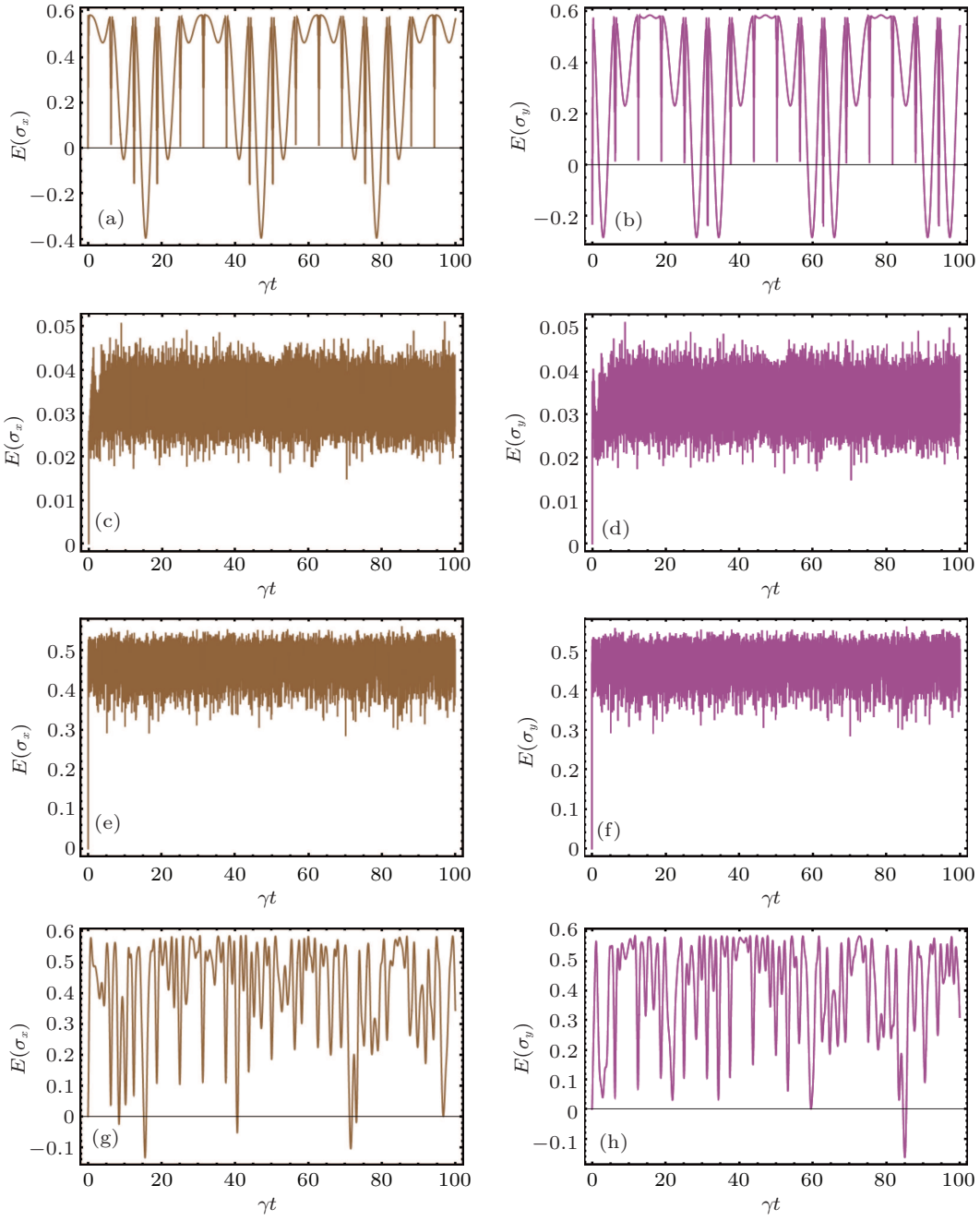


Fig. 4. (color online) Evolution of entropy squeezing versus scaled time γt, here the atom starts in the exited state and the field in a coherent state for $f(n) = \sqrt{n}$, $\mu = 0.1$: (a) $E(\sigma_x)$ with $\langle n\rangle = 25, \Delta = 0, \chi = 0, k = 1, \beta_1 = \beta_2 = 0$; (b) $E(\sigma_y)$ with $\langle n\rangle = 25, \Delta = 0, \chi = 0, k = 1, \beta_1 = \beta_2 = 0$; (c) $E(\sigma_x)$ with $\langle n\rangle = 25, \Delta = 0, \chi = 0.005, k = 1, \beta_1 = \beta_2 = 0$; (d) $E(\sigma_y)$ with $\langle n\rangle = 25, \Delta = 0, \chi = 0.005, k = 1, \beta_1 = \beta_2 = 0$; (e) $E(\sigma_x)$ with $\langle n\rangle = 25, \Delta = 0, \chi = 0.005, k = 2, \beta_1 = \beta_2 = 1$; (f) $E(\sigma_y)$ with $\langle n\rangle = 25, \Delta = 0, \chi = 0.005, k = 2, \beta_1 = \beta_2 = 1$; (g) $E(\sigma_x)$ with $\langle n\rangle = 1, \Delta = 0, \chi = 0.005, k = 1, \beta_1 = \beta_2 = 0$; (h) $E(\sigma_y)$ with $\langle n\rangle = 1, \Delta = 0, \chi = 0.005, k = 1, \beta_1 = \beta_2 = 0$.

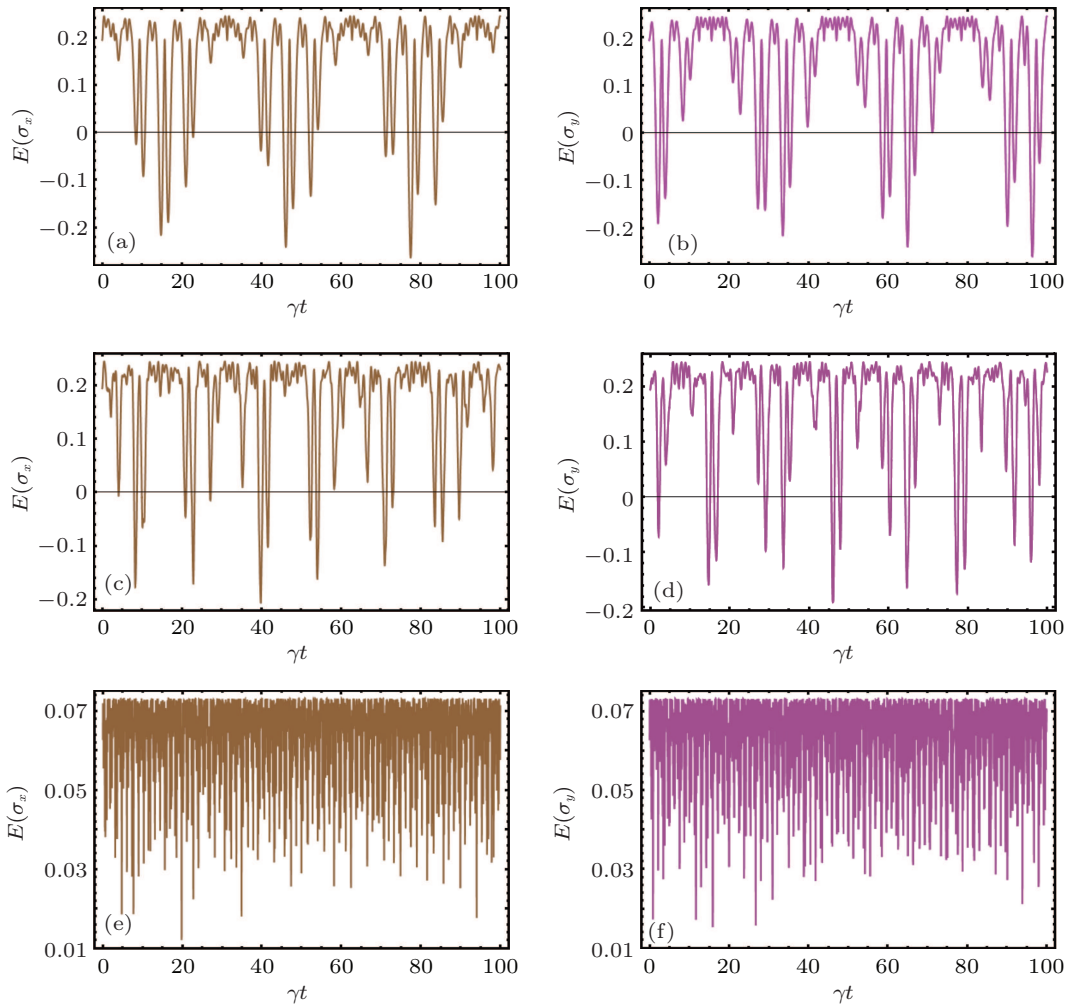


Fig. 5. (color online) Evolution of entropy squeezing versus scaled time γt, here the atom starts in the exited state and the field in a squeezed state for $f(n)=\sqrt{n}, \mu=0.1, \langle n\rangle=1$: (a) $E(\sigma_x)$ with $\Delta=0, \chi=0, k=1, \beta_1=\beta_2=0$; (b) $E(\sigma_y)$ with $\Delta=0, \chi=0, k=1, \beta_1=\beta_2=0$; (c) $E(\sigma_x)$ with $\Delta=0, \chi=0.005, k=1, \beta_1=\beta_2=0$; (d) $E(\sigma_y)$ with $\Delta=0, \chi=0.005, k=1, \beta_1=\beta_2=0$; (e) $E(\sigma_x)$ with $\Delta=0, \chi=0.005, k=2, \beta_1=\beta_2=1$; (f) $E(\sigma_y)$ with $\Delta=0, \chi=0.005, k=2, \beta_1=\beta_2=1$.

6. Discussion on the effect of three- and four-photon transitions

We have investigated the influence of one- and two-photon transitions on the temporal behavior of atomic inversion and entropy squeezing in the previous sections. In this section, we discuss the effect of three- and four-photon transition processes on the time evolution of the mentioned physical quantities in a general manner. Obviously, adding all of the numerical results and related figures considering all quantities with $k=3,4$ will make the paper dramatically large. Therefore, we present our obtained results qualitatively and make a comparison with the previous results for $k=1,2$. Clearly, due the numerous parameters involved in the calculations, we can not reach a sharp result, so our discussion is restricted to the particular parameters used. According to our calculations for $k=3$ and $k=4$ (not shown here), the following results are extracted.

The collapse and revival phenomena exist in a clear manner for three- and four-photon transitions in the linear regime ($f(n)=1$) when the field is initially in the coherent state. As we observed, by increasing the number of photon transitions, the time interval between subsequent revivals will be decreased. In addition, the revival time becomes shorter when the number of photon transitions is increased. This outcome is consistent with the results of Ref. [18]. Moreover, for $k=3,4$, no clear collapse–revival phenomenon is observed for the atom–field state in the linear regime ($f(n)=1$) when the initial field state is squeezed or a thermal state.

The temporal behavior of atomic inversion for $k=3$ and $k=4$ shows a chaotic behavior for the nonlinear regime ($f(n)=\sqrt{n}$) in all cases. When the initial field is a thermal or coherent state, for the case of $k=1$ in the absence of Kerr medium and detuning, the full collapses and revivals are observed in the evolution of atomic inversion.

Our results show that, the Kerr medium has a negligible effect on the time variation of atomic inversion for all cases with $k=3,4$. We observe that in the linear case with $k=3$,

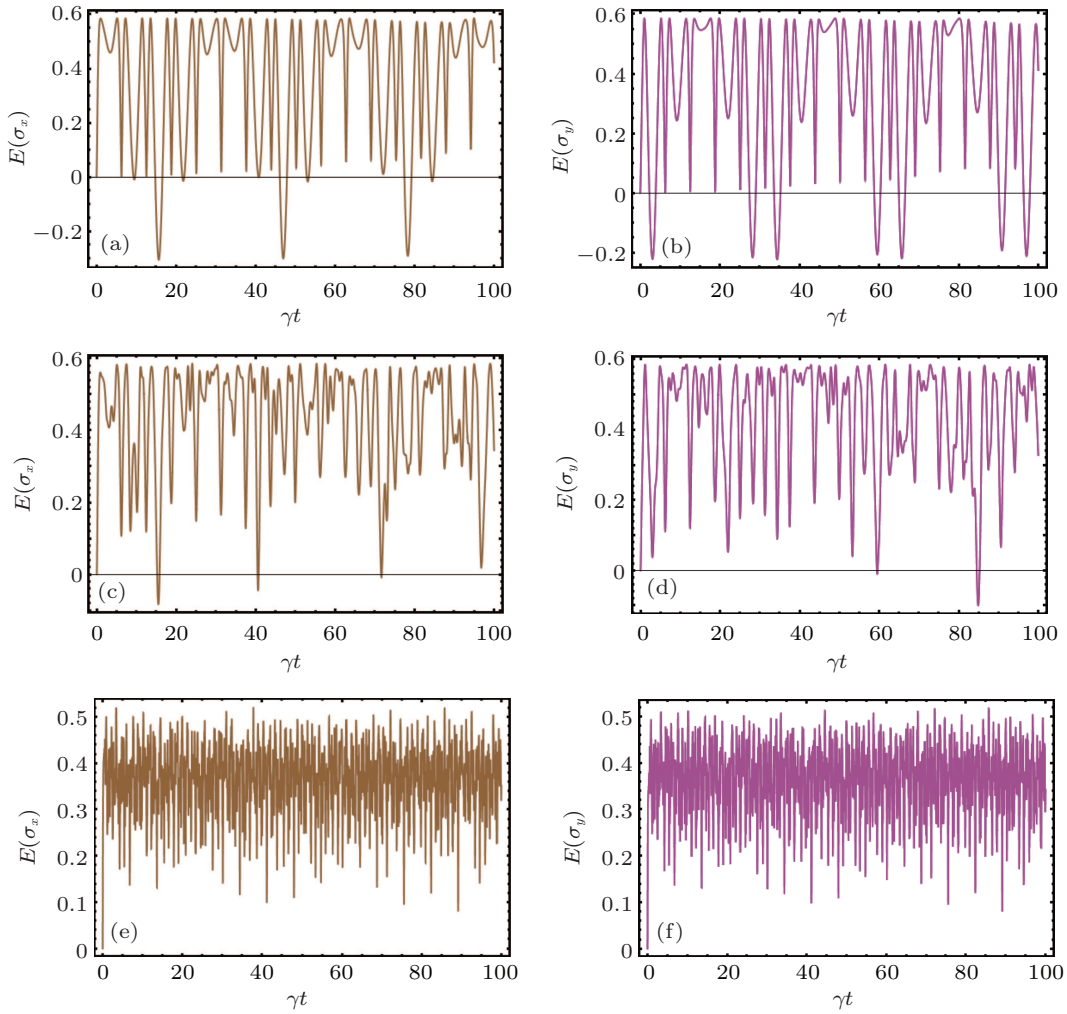


Fig. 6. (color online) Evolution of atomic inversion versus scaled time γt, where a thermal state is used as the initial state of the field. The parameters used in panels (a)–(f) are the same as those in Fig. 5.

the detuning has no critical effect when the coherent or thermal state is the initial field state, while for the squeezed initial state, the negative values of atomic inversion are considerably decreased, i.e., the atomic inversion obtains a positive value most of the time. The same statement is weakly true for the case of $k = 4$.

In the nonlinear case ($f(n) = \sqrt{n}$), there is no (entropy) squeezing in σ_x and σ_y for $k = 4$ with the different initial field states considered in this paper. The situation is the same for the case of $k = 3$ with squeezed and thermal states as the initial states of the field, except, in the absence of the Kerr medium where squeezing occurs in σ_y in a few (very short) intervals of time when the initial field state is coherent. In this latter case, there is no squeezing in σ_x.

7. Summary and conclusions

In this paper, we considered the full nonlinear interaction between a two-level atom and a nonlinear single-mode quantized field for k-photon transitions in the presence of a Kerr medium and the Stark shift effect. We have assumed that the coupling between the atom and the field is time-dependent as well as intensity-dependent. To the best of our knowledge, the problem in such a general form has not been considered in the literature up to now. Fortunately, we could solve the dynamical problem and found the explicit form of the state vector of the whole atom–field system analytically. We have considered the atom to be initially in the exited state and the field in three different possible states (the coherent state, squeezed state and thermal state). The time variations of atomic inversion and entropy squeezing have been numerically studied and compared with each other. Even though our formalism can be used for any nonlinearity function, we particularly considered the nonlinearity function $f(n) = \sqrt{n}$ for our further numerical calculations. The obtained results are summarized as follows. 1) The temporal evolutions of both atomic inversion and entropy squeezing are generally sensitive to the initial field state, and this fact is more visible for the atomic inversion in comparison with entropy squeezing. 2) The behavior of atomic inversion in the presence of nonlinearity (the right plots in all figures) is chaotic, except for some cases, i.e., Figs. 1(b),

2(b) and 3(b), in which the Kerr and the Stark effects are absent and the initial field state is a coherent state, a squeezed state and a thermal state, respectively. As is observed, the collapse and revival phenomena are revealed in Figs. 1(b) and 3(b). 3) The complete (partial) collapse and revival, as purely quantum mechanical features, are observed in the left plots of Fig. 1 (Fig. 3), corresponding to atomic inversion for the initial coherent (thermal) state. 4) The detuning parameter does not have a critical effect on the atomic inversion, unless it causes some minor changes in the extremes of the investigated quantities, either with a chaotic or collapse–revival behavior. 5) The variation of atomic inversion for different initial field states (the coherent, squeezed and thermal states) shows that the time-dependent coupling leads to a time delay which is twice the delay for the time-independent case. This result is similar to the results reported in Ref. [34]. 6) There is entropy squeezing in σ_x and σ_y at some intervals of time in some cases with different conditions, and obviously for different time intervals, such that the uncertainty relation holds. 7) The presence of both the Stark shift and a Kerr medium simultaneously on the entropy squeezing for all cases (different initial field states) prevents the entropy squeezing occurring. 8) In the absence of Kerr medium, Stark shift and detuning with constant coupling ($f(n) = 1$ and $\mu = 0$), and by using the parameters in Ref. [18], our numerical results successfully recover the results in Ref. [18]. In the absence of the mentioned effects with intensity-dependent and time-independent coupling ($f(n) = \sqrt{n}$, $\mu = 0$), our results are reduced to the ones reported in Ref. [45]. 9) As previously mentioned, we have nonlinearized the atom–field system which has been considered in Ref. [34]. Consequently, as is expected, in the linear case ($f(n) = 1$), the results are the same as those in Ref. [34]. Finally, we would like to mention that, our presented formalism has the potential to be applied for all well-known nonlinearity functions, such as the center of mass motion of a trapped ion,[46] photon-added coherent states,[47,48] deformed photon-added coherent states,[49] harmonious states,[39,50] q-deformed coherent states,[25,51–53] etc. We have not discussed the effect of the initial field photon number in detail. It is obvious that the results may be affected directly by this parameter as well as all discussed parameters.

Acknowledgment

The authors would like to thank Dr M J Faghihi for useful discussions.

References

[1] Jaynes E T and Cummings F W 1963 *Proc. IEEE* **51** 89
[2] Huang Y X and Guo G C 1996 *Chin. Phys.* **5** 901
[3] Scully M O and Zubairy M S 1997 *Quantum Optics* (Cambridge: Cambridge University Press)
[4] Setare M R and Barzanjeh Sh 2009 *Chin. Phys. Lett.* **26** 094211
[5] Bužek V, Moya-Cessa H, Knight P L and Phoenix S J D 1992 *Phys. Rev. A* **45** 8190
[6] Ouyang X C, Fang M F, Kang G D, Deng X J and Huang L Y 2010 *Chin. Phys. B* **19** 030309
[7] Tan L, Zhang Y Q and Zhu Z H 2011 *Chin. Phys. B* **20** 070303
[8] Mandel L 1979 *Opt. Lett.* **4** 205
[9] Mirzaee M and Kamani N 2013 *Chin. Phys. B* **22** 094203
[10] Xie R H, Zou Y T and Liu D H 1996 *Chin. Phys. Lett.* **13** 432
[11] Fang M F, Zhou P and Swain S 2009 *J. Mod. Opt.* **47** 1043
[12] Zhang J, Bin S and Zou J 2009 *Chin. Phys. B* **18** 1517
[13] Phoenix S J D and Knight P L 1988 *Ann. Phys.* **186** 381
[14] Kayham H 2011 *Phys. Scr.* **84** 045401
[15] Liao Q, Fang G, Wang Y, Ahmad M A and Liu S 2011 *Optik.* **122** 1392
[16] Zhang J, Wang J and Zhang T 2007 *Opt. Commun.* **277** 353
[17] Mortezapour A, Kordi Z and Mahmoudi M 2013 *Chin. Phys. B* **22** 060310
[18] Kang D P, Liao Q H, Ahamd M A, Wang Y Y and Liu S T 2010 *Chin. Phys. B* **19** 014206
[19] Ateto M S 2010 *Int. J. Theor. Phys.* **49** 276
[20] Buck B and Sukumar C V 1981 *Phys. Lett. A* **81** 132
[21] Sukumar C V and Buck B 1981 *Phys. Lett. A* **83** 211
[22] Bužek V 1989 *Phys. Rev. A* **39** 3196
[23] Faghihi M J and Tavassoly M K 2012 *J. Phys. B: At. Mol. Opt. Phys.* **45** 035502
[24] Sántos-Sanchez O de los and Récamier J 2012 *J. Phys. B: At. Mol. Opt. Phys.* **45** 015502
[25] Naderi M H, Soltanolkotabi M and Roknizadeh R 2004 *J. Phys. Soc. Jpn.* **73** 2413
[26] Barzanjeh S, Naderi M H and Soltanolkotabi M 2010 *J. Phys. A: Math. Theor.* **43** 375304
[27] Abdel-Aty M, Abdalla M S and Obada A S F 2001 *J. Phys. A: Math. Gen.* **34** 9129
[28] Cordero S and Récamier J 2011 *J. Phys. B: At. Mol. Opt. Phys.* **44** 135502
[29] Honarasa G R and Tavassoly M K 2012 *Phys. Scr.* **86** 035401
[30] Faghihi M J, Tavassoly M K and Hooshmandasl M R 2013 *J. Opt. Soc. Am. B* **30** 1109
[31] Faghihi M J and Tavassoly M K 2013 *J. Opt. Soc. Am. B* **30** 2810
[32] Faghihi M J and Tavassoly M K 2013 *J. Phys. B: At. Mol. Opt. Phys.* **46** 145506
[33] Obada A S F, Hanoura S A and Eied A A 2013 *Laser Phys.* **23** 025201
[34] Abdalla M S, Obada A S F and Abdel-khalek S 2008 *Chaos Soliton. Fract.* **36** 405
[35] Puri R R and Bullough R K 1988 *J. Opt. Soc. Am. B* **5** 2021
[36] Ahmad M M A, Khalil E M and Obada A S F 2005 *Opt. Commun.* **257** 76
[37] Obada A S F, Ahmad M M A, Khalil E M and Ali S I 2013 *Opt. Commun.* **287** 215
[38] Liao Q H, Muhammad A A, Wang Y Y and Liu S T 2010 *Commun. Theor. Phys.* **53** 931
[39] Man ko V I, Marmo G, Sudarshan E C G and Zaccaria F 1997 *Phys. Scr.* **55** 528
[40] de Matos Filho R L and Vogel W 1996 *Phys. Rev. A* **54** 4560
[41] Agarwal G S and Singh S 1982 *Phys. Rev. A* **25** 3195
[42] Wolfang P 2000 *Quantum Optics in Phase Space* (Berlin: Wiley-VCH)
[43] Huang C, Tang L, Kong F, Fang J and Zhou M 2006 *Physica A* **368** 25
[44] Fink J M, Göppl M, Baur M, Bianchetti R, Leek P J, Blais A and Wallraff A 2008 *Nature* **454** 315
[45] Li C X and Fang M F 2003 *Chin. Phys.* **12** 0294
[46] de Matos Filho R L and Vogel W 1998 *Phys. Rev. A* **58** R1661
[47] Agarwal G S and Tara K 1991 *Phys. Rev. A* **43** 492
[48] Sivakumar S 1999 *J. Phys. A: Math. Gen.* **32** 3441
[49] Safaeian O and Tavassoly M K 2011 *J. Phys. A: Math. Theor.* **44** 225301
[50] Sudarshan E C J 1963 *Phys. Rev. Lett.* **10** 277
[51] Macfarlane A J 1989 *J. Phys. A: Math. Gen.* **22** 4581
[52] Biedenharn L C 1989 *J. Phys. A: Math. Gen.* **22** L873
[53] Chaichian M and Kulish P 1990 *Phys. Lett. B* **234** 72